Available online at www.sciencedirect.com
SCIENCE DIRECT®

Polymer 46 (2005) 11165–11173

polymer

www.elsevier.com/locate/polymer

Cationic phenyl-substituted poly(*p*-phenylenevinylene) related copolymers with efficient photoluminescence and synthetically tunable emissive colors

Qu-Li Fan[a], Guang-Wei Zhang[a], Xiao-Mei Lu[a,b], Yi Chen[a], Yan-Qin Huang[a], Ying Zhou[a], Hardy Sze On Chan[b], Yee-Hing Lai[b], Guo-Qin Xu[b], Wei Huang[a,*]

[a]*Institute of Advanced Materials (IAM), Fudan University, 220 Handan Road, Shanghai 200433, People's Republic of China*
[b]*Department of Chemistry, National University of Singapore, 3 Science Drive, Singapore 117543, Singapore*

Received 16 May 2005; received in revised form 8 August 2005; accepted 26 August 2005
Available online 13 September 2005

Abstract

A series of amino-functionalized phenyl-substituted poly(*p*-phenylenevinylene) (PPV) related copolymers were synthesized by Wittig reaction. Their corresponding cationic conjugated polymers were successfully obtained via a post-polymerization approach. On the basis of FT-IR and ^{1}H NMR spectra, it was found that phenyl-substituted PPV related copolymers containing alkoxylated benzene (neutral polymer **P1** and quaternized polymer **P1′**), phenylated benzene (neutral polymer **P2** and quaternized polymer **P2′**) and fluorene (neutral polymer **P3** and quaternized polymer **P3′**) moieties are of 55, 80, and 45% *cis*-vinylic linkage respectively while the polymer containing thiophene moiety (neutral polymer **P4** and quaternized polymer **P4′**) is primarily of *trans*-vinylic linkage. Their photoluminescence (PL) were conveniently tuned from blue color to yellow color by introducing units with different optoelectronic properties into the PPV backbones. The polymer with fluorene unit and bulky phenylene-substituted benzene unit in the backbone exhibited the highest PL efficiency among these neutral and quaternized PPVs. **P4′** containing little *cis*-vinylic linkage showed complete quenching while **P1′**–**P3′** containing much more *cis*-vinylic linkage showed incomplete quenching, indicating that the quenching behavior of these cationic PPVs may be highly influenced by the content of *cis*-vinylic linkage in the PPV backbones.

Keywords: Cationic conjugated polymer; Poly(*p*-phenylenevinylene); Fluorescence quenching

1. Introduction

Poly(*p*-phenylenevinylene) (PPV) and its derivatives have attracted a great deal of attention in recent years because of their interesting electroluminescent properties and their potential application as the active emitting layer in light-emitting diodes (LEDs) [1]. Recently, considerable research has focused on anionic PPVs (mainly sulfonated PPVs), which are the good candidates as chemo or biosensors that exhibit rapid and collective response to relatively small perturbations in local environments [2–6]. Such amplified fluorescence quenching is achieved by electron transfer or energy transfer due to the facile energy migration along the conjugated backbone and the relatively strong electrostatic binding of the oppositely charged quenchers with ionic conjugated polymers [7]. Although anionic PPVs exhibit remarkable optoelectronic properties and have been reported on detecting proteins for biological target by electron transfer [2], these polymers suffer from their intrinsic shortcomings such as relatively low photoluminescence (PL) quantum efficiency and their anionic charges that cannot be used to detect anionic biomolecules by electrostatic attraction.

Most recently, cationic fluorescent conjugated polymers were successfully developed to analyze anionic quencher [8] and anionic DNA [9–13] by energy transfer. To obtain highly efficient energy transfer and therefore improve the sensitivity, new types of cationic conjugated polymers with suitable emission wavelength and high PL efficiency are

---

* Corresponding author. Tel.: +86 21 5566 4188; fax: +86 21 6565 5123.
E-mail address: wei-huang@fudan.edu.cn (W. Huang).

0032-3861/$ - see front matter © 2005 Elsevier Ltd. All rights reserved.
doi:10.1016/j.polymer.2005.08.066

required. PPV is very appropriate for the color tunability over the full visible range by the control of its HOMO–LUMO band gap and for enhancement of the PL quantum efficiency under introduction of bulky group into the side chain or incorporation of unit with high PL efficiency into the conjugated main chain [1]. Therefore, it is crucial to develop cationic PPVs with higher PL quantum efficiency and different emission wavelength to evaluate a variety of polymer compositions for obtaining optimized sensory materials.

In this paper, we report the successful syntheses of cationic phenyl-substituted PPV related copolymers. Their emissive color was tuned by introducing arene units with different electronic properties. Furthermore, we attempted

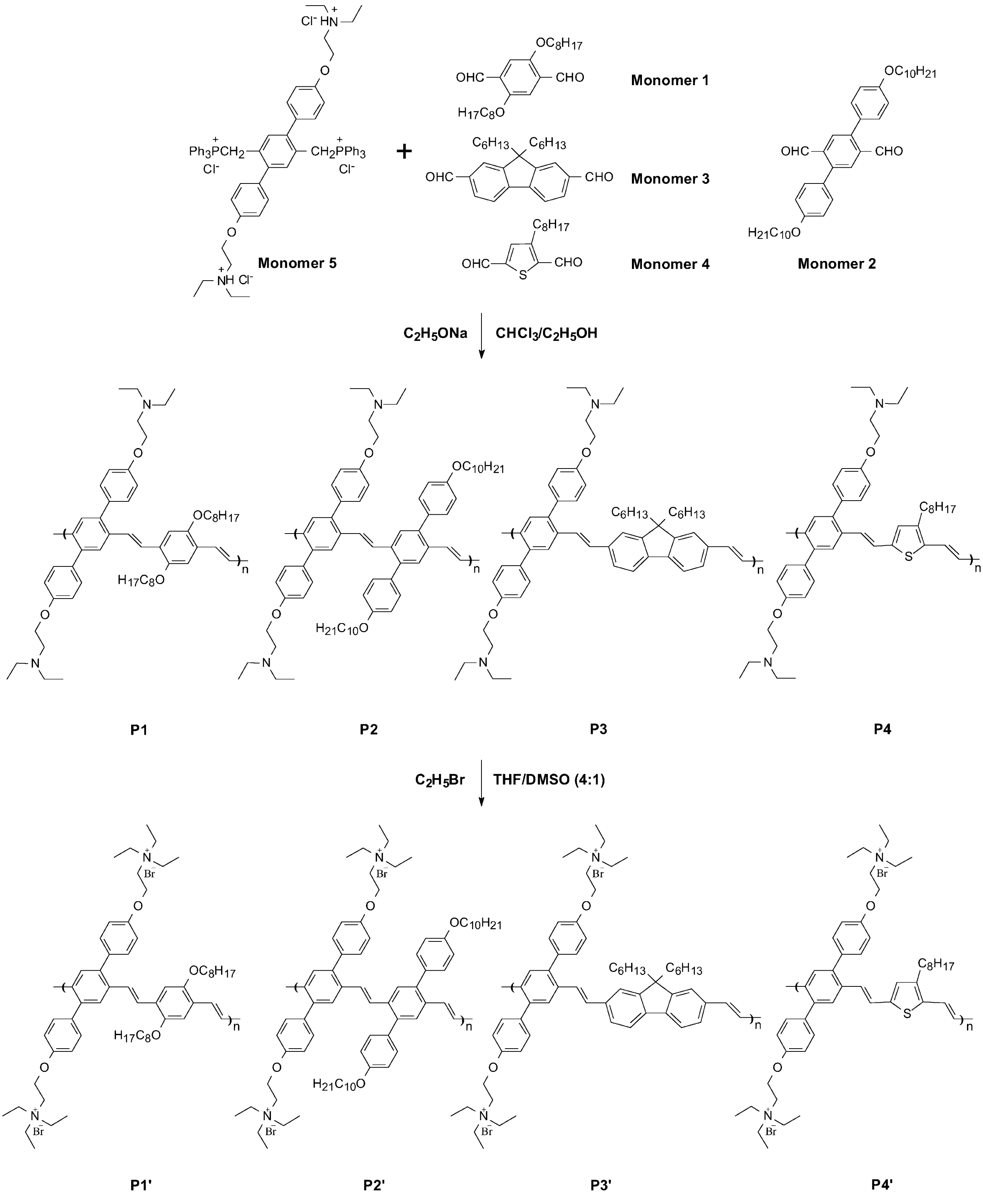

Scheme 1. The synthetic routes for the neutral and quaternized polymers.

to gain highly PL quantum efficiency by incorporating the bulky substituent and the fluorene unit. Phenyl-substituted PPV derivatives are desired as they have proven to exhibit highly efficient fluorescence and enhanced photostability due to the steric hindrance of the bulky phenyl groups which minimize the interchain or intrachain interactions [14–17]. Recently, we have synthesized a type of fully phenyl-substituted cationic PPVs and indeed they strongly blocked the interchain π-stacking in aqueous solution [18]. The fluorene unit is well known as a highly PL efficient unit and has been introduced to enhance the PL efficiency of PPV derivatives [19]. The quenching behavior of these cationic polymers with an anionic quencher $Fe(CN)_6^{4-}$ was also investigated.

2. Experimental

2.1. Materials and synthesis

All chemical reagents used were purchased from Aldrich Chemical Co. THF was purified by distillation in the presence of sodium. Other organic solvents were used without any further purification. The synthetic routes for those neutral and quaternized polymers are shown in Scheme 1.

*2.1.1. 2,5-dioctyloxy-1,4-diformylbenzene (Monomer **1**)*
The compound was synthesized according to Ref. [19].

*2.1.2. 2,5-bis(4′-decyloxyphenyl)-1,4-diformylbenzene (Monomer **2**)*
This compound was synthesized according to Ref. [18].

*2.1.3. 2,7-diformyl-9,9-di-n-hexylfluorene (Monomer **3**)*
The compound was synthesized according to Ref. [19].

*2.1.4. 2,5-diformyl-3-octylthiophene (Monomer **4**)*
The compound was synthesized according to Ref. [20].

*2.1.5. {2,5-bis[4′-2-(N,N-diethylamino)ethoxyphenyl]-1,4-xylene}bis(triphenylphosphonium chloride) dihydrochloride (Monomer **5**)*
This compound was synthesized according to Ref. [18].

2.1.6. General procedure for the preparation of neutral polymers by Wittig Reaction
A solution of 0.476 g (7.0 mmol) of sodium ethoxide in 7 mL of anhydrous ethanol was added to a stirred solution of 1.00 g (0.87 mmol) of triphenylphosphonium chloride Monomer **5** and 0.87 mmol of diformyl monomer (0.338 g of Monomer **1**, 0.338 g of Monomer **3** or 0.218 g Monomer **4**) in 10 mL of dry chloroform and 10 mL of anhydrous ethanol. The mixture was stirred for 12 h and then poured into 200 mL of methanol. The green powder was collected by filtration and further purified by a Soxhlet extraction in methanol for 3 days.

*2.1.6.1. Poly{2,5-bisoctyl-p-phenylenevinylene-alt-2,5-bis[4′-2-(N,N-diethylamino)ethoxyphenyl]-1,4-phenylene-vinylene} (**P1**).* 0.48 g (yield 65%). ^{1}H NMR ($CDCl_3$, ppm): δ 7.83–7.61 (br, Ar-*H*), 7.59–7.07 (br, Ar-*H* and *trans*-vinyl protons), 7.07–6.67 (br, Ar-*H*), 6.61–6.36 (br, *cis*-vinyl protons), 4.24–3.77 (br, $–OCH_2–$), 3.60–3.37 (br, $–OCH_2–$ (connecting to benzene unit directly) in *cis*-vinyl protons), 3.10–2.80 (br, $–OCH_2CH_2N–$), 2.80–2.52 (br, $–NCH_2CH_3$), 1.87–1.61 (br, $–CH_2–$), 1.61–0.98 (br, $–CH_2–$), 0.98–0.65 (br, $–CH_3–$). ^{13}C NMR ($CDCl_3$, ppm): δ 158.72, 151.50, 150.85, 140.10, 139.35, 138.80, 135.55, 133.70, 133.15, 131.90, 131.50, 130.80, 128.00, 126.70, 125.20, 114.56, 69.27, 67.06, 52.24, 48.23, 32.21, 32.11, 29.60, 26.44, 23.01, 14.45, 12.36. FT-IR (KBr pellet, cm^{-1}): 3437 (br), 3030, 2959, 2927, 2856, 2810, 1678, 1516, 1472, 1422, 1382, 1291, 1243, 1203, 1176, 1111, 1031, 973, 914, 873, 833, 723, 652, 544. Anal. Calcd for $(C_{56}H_{78}N_2O_4)_n$: C, 79.77; H, 9.32; N, 3.32. Found: C, 78.49; H, 8.81; N, 2.86.

*2.1.6.2. Poly{2,5-bis(4′-decyloxyphenyl)-1,4-phenylenevinylene-alt-2,5-bis[4′-2-(N,N-diethylamino)ethoxyphenyl]-1,4-phenylenevinylene} (**P2**).* The data were reported in our previous work [18].

*2.1.6.3. Poly{9,9-n-dihexyl-2,7-fluorenediyl-vinylene-alt-2,5-bis[4′-2-(N,N-diethylamino)ethoxyphenyl]-1,4-phenylenevinylene} (**P3**).* 0.51 g (yield 70%). ^{1}H NMR ($CDCl_3$, ppm): δ 8.01–6.91 (br, Ar-*H* and *trans*-vinyl protons), 6.90–6.61 (br, Ar-*H*), 6.61–6.42 (br, *cis*-vinyl protons), 4.35–4.08 (br, $–OCH_2–$ in *trans*-vinyl protons), 4.08–3.90 (br, $–OCH_2–$ in *cis*-vinyl protons), 3.11–2.91 (br, $–OCH_2CH_2N–$ in *trans*-vinyl protons), 2.91–2.79 (br, $–OCH_2CH_2N–$ in *cis*-vinyl protons), 2.79–2.54 (br, $–NCH_2CH_3$), 2.13–1.57 (br, $–CH_2–$), 1.24–0.84 (br, $–CH_2–$), 0.84–0.45 (br, $–CH_3$). ^{13}C NMR ($CDCl_3$, ppm): δ 158.62, 152.02, 141.10, 140.31, 137.20, 136.51, 135.35, 133.40, 131.50, 130.53, 128.00, 125.14, 122.02, 120.27, 114.59, 67.06, 55.21, 52.26, 52.15, 48.27, 41.10, 31.78, 30.11, 24.17, 22.99, 14.35, 12.29. FT-IR (KBr pellet, cm^{-1}): 3437 (br), 3031, 2963, 2926, 2856, 2810, 1681, 1606, 1574, 1518, 1466, 1378, 1290, 1242, 1175, 1049, 1031, 965, 914, 878, 831, 742, 651, 540. Anal. Calcd for $(C_{59}H_{74}N_2O_2)_n$: C, 84.04; H, 8.85; N, 3.32. Found: C, 83.06; H, 8.66; N, 3.35.

*2.1.6.4. Poly{3-octyl-2,5-thiophenediyl-vinylene-alt-2,5-bis[4′-2-(N,N-diethylamino)ethoxyphenyl]-1,4-phenylene-vinylene} (**P4**).* 0.25 g (yield 41%). ^{1}H NMR ($CDCl_3$, ppm): δ 7.80–6.00 (br, Ar-*H* and *trans*/*cis*-vinyl protons), 4.30–3.50 (br, $–OCH_2–$), 3.10–2.30 (br, $–OCH_2CH_2N–$ and $–NCH_2CH_3$), 2.00–1.76 (br, $–ArCH_2–$), 1.70–0.95 (br, $–CH_2–$), 0.98–0.75 (br, $–CH_3$). ^{13}C NMR (CDCl3, ppm): δ 158.74, 158.57, 140.10–132.00 (m), 131.19, 131.01, 130.10–121.00 (m), 114.62, 67.02, 52.26, 48.26, 32.26, 31.24, 29.82, 29.65, 28.81, 23.03, 14.47, 12.33. FT-IR (KBr pellet, cm^{-1}): 3430 (br), 3030, 2965, 2925, 2854, 2809, 1656, 1608, 1574, 1516, 1476, 1379, 1291, 1246, 1174, 1111, 1029, 958, 913, 879, 832, 731, 653, 537. Anal. Calcd for $(C_{46}H_{60}N_2O_2S)_n$: C, 78.36; H, 8.58; N, 3.97; S, 4.55. Found: C, 76.98; H, 8.97; N, 3.82; S, 5.06.

2.1.7. General procedure for the preparation of cationic polymers via post-quaternization on neutral polymers

A 50 mL round-bottom flask with a magnetic spin bar was charged with 0.40 mmol of neutral polymer (0.337 g for **P1**, 0.337 g for **P3** or 0.282 g for **P4**) dissolved in 20 mL of THF. To this was added bromoethane (0.436 g, 4 mmol) and 5 mL of DMSO. The solution was stirred at 50 °C for 3 days and then most of the bromoethane and THF was evaporated. Polymer was precipitated in 100 mL of acetone, collected by centrifugation and dried overnight in vacuum at 50 °C.

*2.1.7.1. Poly-{2,5-bisoctyl-p-phenylenevinylene-alt-2,5-bis[4′-2-(N,N,N-triethylammonium)ethoxyphenyl]-1,4-phenylenevinylene}dibromide (**P1′**).* 0.31 g (yield 72%). ^{1}H NMR ($CDCl_3$, ppm): δ 7.85–6.15 (br, Ar-*H* and vinyl protons), 4.68–4.19 (br, –OCH_2–), 4.07–3.07 (br, –OCH_2– and –NCH_2–), 2.00–0.50 (br, –CH_2– and –CH_3). ^{13}C NMR ($CDCl_3$, ppm): δ 157.57, 151.05, 140.10, 135.93, 134.75, 131.34, 130.77, 130.05, 128.00, 114.71, 69.57, 62.78, 61.95, 56.32, 54.14, 51.42, 31.94, 29.39, 26.39, 22.70, 13.55, 8.33, 7.08. FT-IR (KBr pellet, cm^{-1}): 3429 (br), 3040, 2954, 2926, 2854, 2640, 2475, 1670, 1514, 1469, 1418, 1383, 1286, 1239, 1201, 1112, 1178, 1112, 1026, 970, 940, 874, 833, 721, 660, 544. Anal. Calcd for $(C_{56}H_{78}N_2O_4\cdot 1.9C_2H_5Br\cdot 2H_2O)_n$: C, 66.12; H, 8.49; N, 2.58; Br, 13.98. Found: C, 64.23; H, 7.66; N, 2.22, Br, 15.86. The water present in the elemental analysis results was based on mass loss in the TGA [21].

*2.1.7.2. Poly{2,5-bis(4′-decyloxyphenyl)-1,4-phenylenevinylene-alt-2,5-bis[4′-2-(N,N,N-triethylammonium)ethoxyphenyl]-1,4-phenylenevinylene}dibromide (**P2′**).* The data were reported in our previous work [18].

*2.1.7.3. Poly{9,9-n-dihexyl-2,7-fluorenediyl-vinylene-alt-2,5-bis[4′-2-(N,N,N-triethylammonium)ethoxyphenyl]-1,4-phenylenevinylene}dibromide (**P3′**).* 0.32 g (yield 75%). ^{1}H NMR ($CDCl_3$, ppm): δ 7.93–6.15 (br, Ar-*H* and vinyl protons), 4.70–4.14 (br, –OCH_2–), 4.00–3.04 (br, –OCH_2– and –NCH_2–), 2.20–0.25 (br, –CH_2– and –CH_3). ^{13}C NMR ($CDCl_3$, ppm): δ 157.65, 151.76, 141.11, 140.18, 137.22, 134.73, 131.45, 130.82, 130.26, 127.69, 120.07, 114.71, 62.69, 61.86, 56.35, 54.13, 51.49, 40.41, 31.56, 29.63, 23.84, 22.49, 13.40, 8.31, 7.04. FT-IR (KBr pellet, cm^{-1}): 3428 (br), 3030, 2965, 2924, 2853, 2630, 2467, 1680, 1605, 1575, 1514, 1465, 1394, 1287, 1235, 1177, 1060, 1006, 973, 914, 883, 829, 742, 654, 540. Anal. Calcd for $(C_{59}H_{74}N_2O_2\cdot 1.9C_2H_5Br\cdot H_2O)_n$: C, 70.61; H, 8.07; N, 2.62; Br, 14.21. Found: C, 68.69; H, 6.98; N, 2.37, Br, 15.12.

*2.1.7.4. Poly{3-octyl-2,5-thiophenediyl-vinylene-alt-2,5-bis[4′-2-(N,N,N-triethylammonium)ethoxyphenyl]-1,4-phenylenevinylene}dibromide (**P4′**).* 0.24 g (yield 65%). ^{1}H NMR (CD3OD, ppm): δ 7.90–6.10 (br, Ar-*H* and *trans*/*cis*-vinyl protons), 4.70–4.00 (br, –OCH_2–), 4.00–3.00 (br, –OCH_2CH_2N– and –NCH_2CH_3), 2.00–1.00 (br, –$ArCH_2$– and –CH_2– and –NCH_2CH_3), 0.98–0.75 (br, –CH_3). ^{13}C NMR (CD_3OD, ppm): δ 157.54, 140.30–133.10 (m), 131.30, 130.10–126.00 (br), 114.65, 62.63, 61.83 56.30, 54.11, 51.45, 32.00, 30.95, 29.40, 28.03, 22.70, 13.49, 8.31, 7.09. FT-IR (KBr pellet, cm^{-1}): 3437 (br), 3032, 2970, 2924, 2853, 2642, 2472, 1643, 1607, 1574, 1516, 1476, 1390, 1289, 1238, 1178, 1112, 1026, 952, 910, 834, 726, 658, 539. Anal. Calcd for $(C_{46}H_{60}N_2O_2S\cdot 1.9C_2H_5Br\cdot 1.5H_2O)_n$: C, 63.69; H, 7.78; N, 2.98; S, 3.41; Br, 16.17. Found: C, 62.77; H, 7.75; N, 2.67; S, 3.86; Br, 17.50.

2.2. Measurements

The NMR spectra were collected on a Varian Mercury Plus 400 spectrometer with tetramethylsilane as the internal standard. FT-IR spectra were recorded on a Shimadzu IRPrestige-21 FT-IR-8400s spectrophotometer by dispersing samples in KBr. Mass spectra (MS) were obtained using a HP 5973MS mass spectrometer at an ionizing voltage of 70 eV. UV–vis spectra were recorded on a Shimadzu 3150 PC spectrophotometer. The concentrations of copolymer solutions were adjusted to about 0.01 mg/mL or less. Fluorescence measurement was carried out on a Shimadzu RF-5301 PC spectrofluorophotometer with a xenon lamp as a light source. Thermogravimetric analysis (TGA) was performed on a Shimadzu Thermogravimetry and Differential Thermal Analysis DTG-60H at a heating rate of 10 °C/min under N_2. Elemental microanalyses were carried out on a Vario EL III CHNOS elemental analyzer. Gel permeation chromatography (GPC) analysis was conducted with a HP1100 HPLC system equipped with 7911GP-502 and GP NXC columns using polystyrenes as the standard and tetrahydrofuran (THF) as the eluant at a flow rate of 1.0 mL/min and 35 °C.

The quenching behavior was studied by comparing the fluorescence intensities of polymer methanol solutions in the presence of quenchers with different concentrations. Methanol and Milli-Q water used in preparing the solution of polymers and quenchers was purged with nitrogen for 4 h before using.

3. Results and discussion

3.1. Color and solubility

In all neutral polymers, **P1** is a bright orange solid, **P2** is a bright green solid, **P3** is a bright blue–green solid, and **P4** is a red solid. Compared with those neutral polymers, the obtained quaternized polymers show slightly deeper colors, in which **P1′** is red, **P2′** is yellow–green, **P3′** is green, and **P4′** is deep red. All of the neutral polymers prepared by Wittig reaction are readily soluble in common organic solvents such as chloroform, tetrahydrofuran, 1,2-dichloroethane, etc. but have poor solubility in polar ones such as methanol, DMSO and DMF. **P1′**–**P4′** could be dissolved well in DMSO, DMF, and CH_3OH, indicating enhanced polarity from the formed cationic groups after quaternization.

In addition, the neutral polymers **P1**, **P3** and **P4** exhibited good solubility in acetic acid–methanol, acetic acid-DMSO or acetic acid aqueous solution (1 M). Such an increased solubility of neutral polymers in polar solvent has been reported by our group previously, which is attributed to the interaction between the weak organic acid and the terminal amino group through the electrostatic interaction that could increase the affinity of the polymer with those polar solvents [18,22]. While for **P2**, it could not be dissolved in acetic acid aqueous solution although it showed good solubility in methanol, DMSO, and DMF under acetic acid assistance. It is easy to understand that with the increased content of hydrophobic groups (bulky phenyl groups in all side chains) in **P2**, the acetic acid assistance could not afford enough solubility of **P2** in water.

3.2. FT-IR analysis

Infrared spectra for all polymers were shown in Fig. 1. It can be seen that a weak absorption, which can be attributed to the aldehyde end groups for **P1**–**P4**, appears at 1680 cm^{-1}, indicating incomplete intermolecular condensation. Interestingly, it was also found that the ratio of *trans*–CH=CH (~975 cm^{-1}) linkage to *cis*–CH=CH (~875 cm^{-1}) linkage in the IR spectrum of **P2** was rather different from that of **P1**, **P3** and **P4** [23,24]. A weak absorption peaked at 875 cm^{-1} (*cis*–CH=CH) was clearly visible for **P2** while no signals could be found at 970 cm^{-1} (*trans*–CH=CH), indicating that **P2** predominantly contains *cis*–CH=CH linkage under Wittig conditions. For **P4** with thiophene moiety in the conjugated backbone, on the contrary, a much stronger absorption peaked appeared at 960 cm^{-1} (*trans*–CH=CH) compared with the peak at 876 cm^{-1} (*cis*–CH=CH). Meanwhile, a similar IR absorption intensity of *cis*–CH=CH linkage with *trans*–CH=CH linkage was observed for **P1** and **P3** which were also obtained by Wittig reaction. The ratio of *trans*- vs *cis*-configuration can be determined by ^1H NMR spectrum, which will be discussed in the next section.

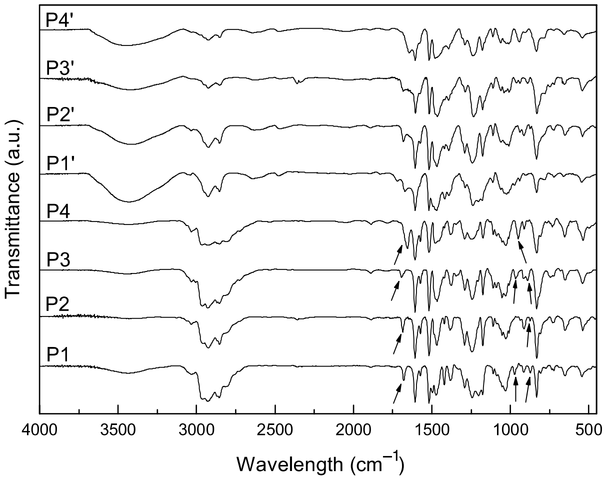

Fig. 1. FT-IR spectra of the neutral and quaternized PPVs.

After quaternization, there are no obvious changes with the position of most peaks but greater changes with the intensity of some peaks compared with their respective neutral polymers (Fig. 1). Besides, a broad and strong self-associated absorption peak of water at 3400 cm^{-1} can be observed, which reflects strong hydrophilicity of the resulting quaternized polymers.

3.3. NMR analysis

^1H NMR spectra of all the neutral and quaternized polymers were shown in Fig. 2. Integration ratios of the end aldehyde protons (10.01 ppm) to the $–OCH_2CH_2N–$ protons for **P1**–**P4** (3.00–2.75 ppm) were found to be about 1/36, 1/30, 1/32, and 1/24, corresponding to 18, 15, 16, and 12 phenyl rings in the backbone, respectively. These results are in good agreement with those measured by GPC (Table 1). Our FT-IR analysis showed that **P2** adopted predominantly *cis*–CH=CH while *trans*–CH=CH dominated in **P4**, and as for **P1** and **P3**, both *cis*–CH=CH and *trans*–CH=CH configurations were present. Such a result was also substantiated by ^1H NMR measurements. The ^1H NMR peaks of all the neutral polymers corresponding to $–OCH_2–$ and $–CH_2N–$ groups split into two parts, in which the downfield and upfield ones were caused by the *trans*- and *cis*-configurations, respectively [23,24]. For **P3**, clear separation between the two resonance signals near 4.2 and 4.0 ppm offered a convenient way to accurately estimate the relative *cis*/*trans*–CH=CH contents. The ratio of *cis*- to *trans*-vinylic linkage for **P1** was determined by comparing

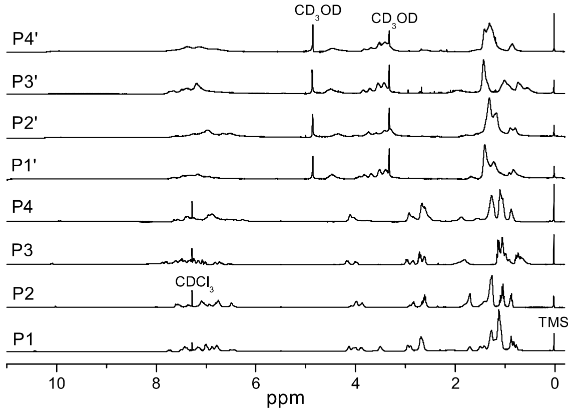

Fig. 2. ^1H NMR spectra of the neutral and quaternized PPVs.

Table 1
GPC and spectroscopic data for all neutral and quaternized polymers

Polymer	GPC			Content of *cis*–CH=CH (%)[a]	Absorbance λ_{max} (nm)	Emission λ_{max} (nm)	Φ_{pl}
	M_n[b]	M_w[b]	PDI[b]				
P1[c]	8300	12,000	1.45	55	437	524	0.40
P2[c]	8600	12,000	1.40	80	392	500	0.55
P3[c]	7400	11,000	1.46	45	397	476	0.80
P4[c]	4200	5300	1.26	$\ll 50$	437	585	0.03
P1′[d]	–	–	–	–	404	508	0.18
P2′[d]	–	–	–	–	370	484	0.28
P3′[d]	–	–	–	–	413	470	0.35
P4′[d]	–	–	–	–	449	551	0.01

[a] The *cis*–CH=CH contents were estimated from the integration of –OCH$_2$– signals in the ^{1}H NMR.

[b] M_n, M_w and PDI of the polymers were determined by gel permeation chromatography using polystyrene standards.

[c] The spectroscopic data of neutral polymers were measured in THF.

[d] Those of quaternized polymers in methanol, using the quinine sulfate solution (ca. 1.0×10^{-5} M) in 0.10 M H$_2$SO$_4$ ($\Phi_f = 55\%$) as a standard.

the relative integrations of the –OCH_2C$_7$H$_{15}$ resonance from *cis*-configuration at 3.50 ppm with the –OCH$_2$CH_2N– resonance between 3.00 and 2.75 ppm. The ratio for **P2** has been reported in our previous work. For **P4**, although the two split peaks which were caused by the *trans*- and *cis*-vinylic linkages on the signals of –OCH$_2$– and –CH$_2$N– groups could be observed, they mixed together and made it difficult to calculate the ratio of *cis*- to *trans*-vinylic linkage. However, it is obvious that the signal of *trans*-vinylic linkage was much stronger than *cis*-vinylic linkage. Combined with the remarkably stronger absorption intensity of *trans*–CH=CH linkage than that of *cis*–CH=CH linkage in FT-IR spectrum, we could estimate the content of *cis*-vinylic linkage in **P4** was significantly lower ($\ll 50\%$). All the results are shown in Table 1.

Such different contents of *cis*- and *trans*-vinylic linkages clearly showed that the formation of *trans*- and *cis*-vinylic linkages via Wittig reaction was determined by the type of arene units we introduced into the PPV backbone. The optoelectronic properties or the chemical structure or other properties of these arene units were supposed to highly influence the Wittig reaction. Further work should be done in the future to investigate this phenomenon.

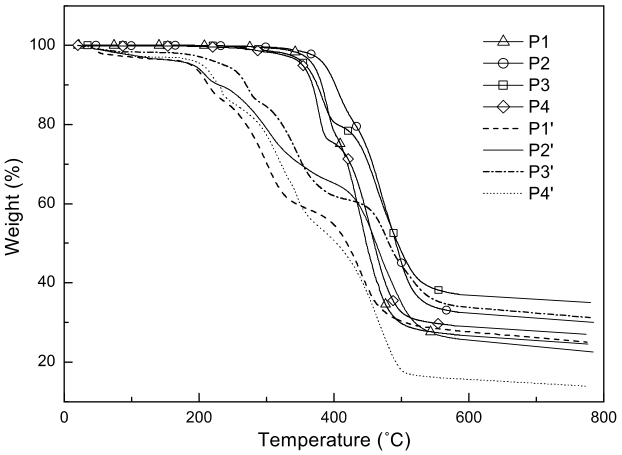

Fig. 3. Thermalgravimetric analysis of the neutral and quaternized PPVs.

As shown in Fig. 2, after quaternization with bromoethane, all proton peaks turns broadened, some of which could not be identified. **P1′**–**P4′** exhibit spectra in which all the signals from –OCH$_2$CH_2N–, –NCH_2CH$_3$ and –NCH$_2$CH_3 groups are downshifted. The quaternization degrees (QD) was determined from the ^{1}H NMR spectra by comparing the relative integrations of the aromatic peaks at 6.0–8.0 ppm (total aromatic and vinyl protons) with that of 0.5–2.0 ppm (total alkyl protons for –OCH$_2$C$_7$$H_{15}$ and –NCH$_2$CH_3 in **P1′**, –OCH$_2$C$_9$$H_{19}$ and –NCH$_2$CH_3 in **P2′**, –C$_6$$H_{13}$ and NCH$_2$CH_3 in **P3′**, and –CH$_2$C$_7$$H_{15}$ and –NCH$_2$CH_3 in **P4′**) [25]. As a result, the QDs of **P1′**, **P2′**, **P3′**, and **P4′** were calculated to be about 95, 90, 95 and 95%, respectively, which were close to the results from elemental analysis.

3.4. Thermal stability

Thermal properties of the polymers were studied by thermogravimetric analysis (TGA) under nitrogen atmosphere. The thermograms in Fig. 3 showed that the neutral polymers **P1**–**P4** exhibited good thermal stability with a weight loss of 3% at 310 °C. For the quaternized samples, the degradation onsets for **P1′**–**P4′** decreased to 200 °C with a small amount of H$_2$O loss at low temperature [21]. This variation can be explained by the lower stability of ethyl bromide than that of the other alkoxy side chains [21]. Although the thermal stability of quaternized polymers decreased, their degradation temperature at nearly 200 °C made them enough serve as chemo or biosensors in room temperature.

3.5. Optical properties

The absorption and emission spectra of the neutral polymers in CHCl$_3$ were shown in Fig. 4. **P1** and **P4** both showed a maximum absorption peak at 437 nm. **P2** and **P3**

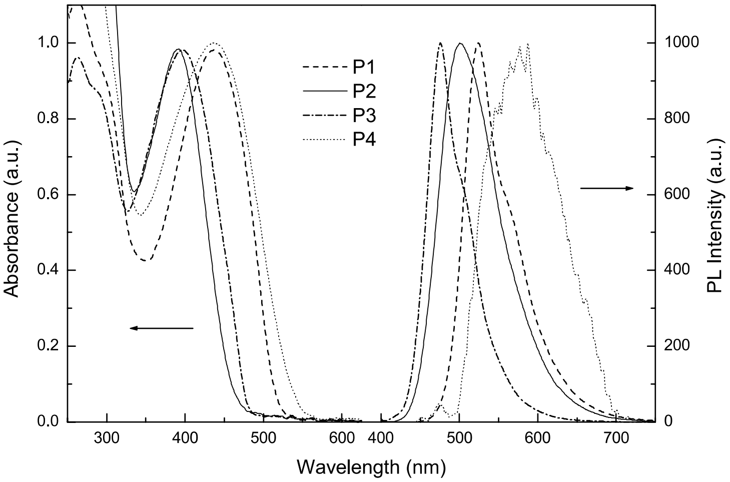

Fig. 4. UV–vis absorption and PL emission spectra of neutral polymers in $CHCl_3$.

showed absorption maxima at 392 and 397 nm, respectively. These blue-shifted UV–vis absorption wavelengths compared to that of MEH-PPV at 510 nm [19] are highly due to the lack of electron-donating ability of the phenyl substituent and the fluorene unit in the alternating copolymer system.

The PL spectra showed an obvious change of emission maxima by the type of substituents and the alternating units in the main chain. In the PL spectra, the effects of phenyl substituent and fluorene unit in the copolymer systems were well consistent with the UV–vis absorption patterns of the polymers. Compared with the emission maximum at 595 nm for MEH-PPV [19], those for **P1**–**P4** were blue-shifted to 524, 500, 476 and 585 nm, respectively. Such different distances of the blue-shifts for the four neutral polymers can be attributed to the alternating units with different electronic properties, in which thiophene and alkoxylated phenyl units are electron rich moieties while phenyl-substituted benzene unit and alklated fluorene unit are electron deficient moieties in the alternating copolymer systems. Furthermore, most of the polymers with phenyl-substituted phenylene unit showed extremely high PL efficiency in solution, which are 40% for **P1**, 55% for **P2** and 80% for **P3** (Table 1). The highly enhanced PL efficiency of **P3** may be due to the non-electron-donating phenyl group [14–17] and the introduction of highly fluorescent fluorene unit in the conjugated main chain [19]. In addition, the emission spectrum of **P1** and **P3** were more featured than that of **P2**, indicating that **P2** emitted with an excited state of more twisted conformation [18]. This may result from its high content of *cis*-vinylic linkage. However, **P4** showed dramatically lower PL efficiency ($\Phi_f = 3\%$) although **P4** also contained phenyl-substituted benzene unit. This might be explained by the existence of thiophene unit with poor light-emitting property in the conjugated backbone [26].

The absorption and emission spectra of the quaternized polymers in methanol were shown in Fig. 5. Quaternization was found to lead to more obvious blue-shifted UV–vis absorption and emission spectra of **P1′** and **P2′**. Such a blue-shift, attributed to the mutual electrostatic repulsion of positive charges pendent on the alternating benzene rings

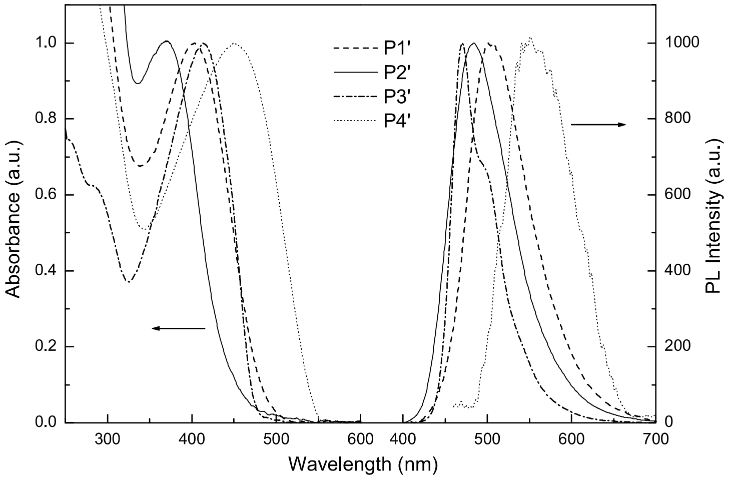

Fig. 5. UV–vis absorption and PL emission spectra of quaternized polymers in methanol.

which leads to an increased torsion of the conjugated main chain and a decreased effective conjugation length, have been reported in other quaternized systems [18,21,22,27]. However, it is intriguing to find that after quaternization **P3′** and **P4′** showed red-shifted absorption maxima at 414 and 449 nm and blue-shifted emission maxima at 470 and 551 nm, respectively. This different shift indicates that the fluorene or thiophene unit, instead of the phenylene unit, in the conjugated main chain might highly influence the interaction of neighboring positive charges and therefore the chain conformation. In addition, just as what we discovered in neutral polymers, the quaternized phenylene-substituted polymers **P4′**, **P1′**, **P2′**, and **P3′** also showed gradual increase of blue-shift of emission maxima compared with anionic PPV (emission maxima at 590 nm) [2], which were 551 nm (greenish yellow), 508 nm (yellowish green), 484 nm (blueish green) and 470 nm (blue), respectively.

Among all quaternized polymers, **P3′** showed the highest Φ_f at 35%, while **P1′** at 18% and **P2′** at 28%, indicating that introducing highly fluorescent fluorene unit into the conjugated backbone surely enhanced the PL efficiency of such cationic PPV system. However, compared with their corresponding neutral polymers, the obvious reduction of PL efficiencies existed in these quaternized phenyl-substituted PPV copolymers. Considering the existence of bulky phenyl group in the polymer side chain and its steric effect on impeding the interchain and intrachain interaction, such PL efficiency decrease may not be simply explained by interchain or intrachain interaction. As we discussed in our previous work [18], it is maybe the non-planarization in the excited state of these cationic polymers that leads to such decreased PL efficiencies [28].

3.6. Quenching behavior

The Stern–Volmer plots of cationic phenyl-substituted PPV related copolymers quenched by $Fe(CN)_6^{4-}$ were shown in Fig. 6. **P1′**–**P3′** displayed downward curves while **P4′** showed an upward curve. Generally, such downward curves were explained by the existence of two populations of fluorophores, one of which was inaccessible to the quencher [29]. With the introduction of a quencher, only those accessible fluorophores were quenched while the fluorescence from the inaccessible ones remained. Thus, there existed inaccessible fluorophores (inaccessible conjugated length) in **P1′**–**P3′** while no inaccessible fluorophore in **P4′**. Considering the much higher contents of *cis*-vinylic linkage in **P1′**–**P3′** than that in **P4′**, their different quenching effect may be highly related to their different content of *cis*- and *trans*-vinylic linkages. Previously, we have investigated the optoelectronic properties of phenyl-substituted PPV derivatives with different contents of *cis*- and *trans*-vinylic linkages [18]. It was showed that the phenyl-substituted PPV derivatives with high content of *cis*-vinylic linkages exhibited more twisted and coiled backbone conformation and shorter effective conjugated length than those with low content of *cis*-vinylic linkages. Thus, some conjugated length might be buried in the twisted and coiled polymer chains with high content of *cis*-vinylic linkages and inaccessible by quenchers. Consequently, it is probable to attribute the inaccessible fluorophore (incomplete quenching) of **P1′**–**P3′** to their high contents of *cis*-vinylic linkage and non-inaccessible florophore (complete quenching) of **P4′** to its low content of *cis*-vinylic linkage. Besides, **P1′** and **P3′** with lower contents of *cis*-vinylic linkage than **P2′** presented higher quenching effects than **P2′**, which further implied that the content of inaccessible fluorophore was related to the content of *cis*-vinylic linkage in PPV derivatives. In this paper, we have known that the formation of *trans*- and *cis*-vinylic linkages via Wittig reaction was determined by the type of arene units we introduced into the PPV backbone. Therefore, the quenching effects of those polymers can be essentially attributed to the properties of those arene units.

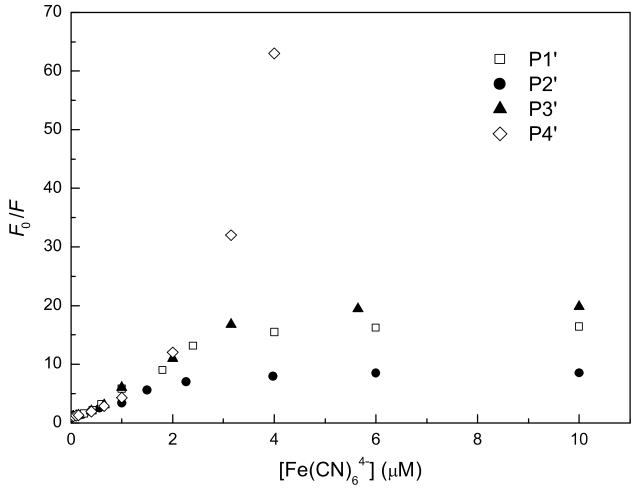

Fig. 6. Stern–Volmer plot of **P1′**–**P4′** (5 μM) quenched by $Fe(CN)_6^{4-}$ in methanol.

4. Conclusions

In this work, we synthesized a series of amino-functionalized phenyl-substituted poly(*p*-phenylenevinylene) related copolymers containing thiophene, fluorene, alkoxylated benzene or phenylated benzene moiety by traditional Wittig reaction. Their corresponding cationic light-emitting polymers were successfully obtained via a post-polymerization approach. From FT-IR and ^{1}H NMR spectra, it was showed that those polymers had different *cis*-vinyl contents, according to their different arene units in the conjugated backbones. Their emissive colors were conveniently tuned from blue to yellow by introducing units with different optoelectronic properties into the PPV conjugated backbone. **P3** and **P3′**, with fluorene unit and bulky phenylene-substituted benzene unit, exhibited the highest PL efficiency among those neutral and quaternized

PPVs. Further investigation showed that **P4′** containing little *cis*-vinyl content showed complete quenching while **P1′**–**P3′** containing much more *cis*-vinyl contents showed incomplete quenching, indicating that the quenching behavior of these cationic PPVs might be highly influenced by the content of *cis*-vinylic linkage in the PPV backbones.

Acknowledgements

This work was financially supported by the National Natural Science Foundation of China under Grants 60325412, 90406021, and 50428303 as well as the Shanghai Commission of Science and Technology under Grants 03DZ11016 and 04XD14002 and the Shanghai Commission of Education under Grant 2003SG03.

References

[1] Mitschke U, Baüerle P. J Mater Chem 2000;10:1471.

[2] Chen L, McBranch DW, Wang HL, Helgeson R, Wudl F, Whitten DG. Proc Natl Acad Sci USA 1999;96:12287.

[3] Gaylord BS, Wang S, Heeger AJ, Bazan GC. J Am Chem Soc 2001;123:6417.

[4] Jones RM, Bergstedt TS, McBranch DW, Whitten DG. J Am Chem Soc 2001;123:6726.

[5] Wang D, Gong X, Heeger PS, Rininsland F, Bazan GC, Heeger AJ. Proc Natl Acad Sci USA 2002;99:49.

[6] Fan C, Plaxco KW, Heeger AJ. J Am Chem Soc 2002;124:5642.

[7] Zhou Q, Swager TM. J Am Chem Soc 1995;117:12593.

[8] Harrison BS, Ramey MB, Reynolds JR, Schanze KS. J Am Chem Soc 2000;122:8561.

[9] Gaylord BS, Heeger AJ, Bazan GC. Proc Natl Acad Sci USA 2002;99:10954.

[10] Gaylord BS, Heeger AJ, Bazan GC. J Am Chem Soc 2003;125:896.

[11] Liu B, Bazan GC. Chem Mater 2004;16:4467.

[12] Gaylord BS, Massie MR, Feinstein SC, Bazan GC. Proc Natl Acad Sci USA 2005;102:34.

[13] Liu B, Bazan GC. Proc Natl Acad Sci USA 2005;102:589.

[14] Spreitzer H, Becker H, Kluge E, Kreuder W, Schenk H, Demandt R, et al. Adv Mater 1998;10:1340.

[15] Wan WC, Antoniadis H, Choong VE, Razafitrimo H, Gao Y, Feld WA, et al. Macromolecules 1997;30:6567.

[16] Hsieh BR, Yu Y, Forsythe EW, Schaaf GM, Feld WA. J Am Chem Soc 1998;120:231.

[17] Peng Z, Zhang J, Xu B. Macromolecules 1999;32:5162.

[18] Fan QL, Lu S, Lai YH, Huang W. Macromolecules 2003;36:6976.

[19] Ahn T, Song SY, Shim HK. Macromolecules 2000;33:6764.

[20] Ding AL, Pei J, Yu WL, Lai YH, Huang W. Thin Solid Films 2002;417:198.

[21] Balanda PB, Ramey MB, Reynolds JR. Macromolecules 1999;32:3970.

[22] Liu B, Yu W, Lai YH, Huang W. Macromolecules 2002;35:4975.

[23] Liao L, Pang Y, Ding L, Karasz FE. Macromolecules 2001;34:6756.

[24] Liao L, Pang Y, Ding L, Karasz FE. Macromolecules 2001;34:7300.

[25] The QDs of **P1′**, **P3′** and **P4′** were calculated according to the following equations: $(42+6x)/16=I_{0.5-2.0}/I_{6.0-8.0}$, $(38+6x)/20=I_{0.5-2.0}/I_{6.0-8.0}$, and $(27+6x)/15=I_{0.5-2.0}/I_{6.0-8.0}$, respectively. Where x is the QD, $I_{0.5-2.0}$ is the integration of the peaks at 0.5–2.0 ppm and $I_{6.0-8.0}$ is the integration of the peaks at 6.0–8.0 ppm. The QD of **P2′** has been reported in our previous work (see Ref. [18])

[26] Mitschke U, Bäuerle P. J Mater Chem 2000;10:1471.

[27] Fan QL, Zhou Y, LU XM, Hou XY, Huang W. Macromolecules 2005;38:2927.

[28] Oelkrug D, Tompert A, Gierschner J, Egelhaaf HJ, Hanack M, Hohloch M, et al. J Phys Chem B 1998;102:1902.

[29] Lakowicz JR. Principles of fluorescence spectroscopy. 2nd ed. New York: Plenum Press; 1999.